SiGe BiCMOS 65-GHz BPSK Transmitter and 30 to 122 GHz LC-Varactor VCOs with up to 21% Tuning Range

C. Lee, T. Yao, A. Mangan, K. Yau, M. A. Copeland*, and S. P. Voinigescu

Edward S. Rogers, Sr. Dept. of Electrical & Computer Eng., University of Toronto, Toronto, ON, M5S 3G4, Canada
* Professor Emeritus, Carleton University, Ottawa, ON, Canada
e-mail: chihou@eecg.toronto.edu

Abstract

This paper presents a systematic study of millimetre-wave, low-noise, widely-tuneable differential Colpitts VCOs. A design methodology was developed and validated experimentally over thirteen different varactor-tuned (VCO) and fixed-frequency L-C oscillators spanning the 30-GHz to 122-GHz frequency range. All circuits employ accumulation-mode n-MOS varactors, and multi-turn on-chip inductors. The 35-GHz and 60-GHz oscillators achieve phase noise of -112.7 dBc and -104 dBc/Hz, respectively at 1-MHz offset and deliver +4 dBm differential output power while a push-push implementation demonstrates 15-GHz (21%) tuning range from 63.5 GHz to 78.5 GHz. A directly-modulated, 65-GHz binary phase shift keying (BPSK) transmitter is also implemented.

INTRODUCTION

Integrated millimeter-wave voltage controlled oscillators (VCOs) with significant output power, low phase noise, and wide tuning range are crucial to realizing advanced communication and radar systems. Integrating the VCO with other mm-wave transceiver building blocks is becoming a viable option in leading edge SiGe bipolar technologies, thereby reducing cost, size, and improving performance. This paper presents a family of mm-wave VCOs and a 65-GHz binary phase shift keying (BPSK) transmitter which, together with a recently-reported 52-GHz LNA [1], serve as part of a 60-GHz WLAN chip set fabricated in a commercial 0.18μm SiGe BiCMOS technology [2]. Unlike in other mm-wave SiGe-HBT circuits [3,4], accumulation-mode n-MOS (as opposed to p-n junction) varactors and multi-turn inductors [5] (as opposed to transmission-lines) are employed to achieve a sufficiently wide tuning range and low phase noise while minimizing die area.

CIRCUIT CONCEPTS

The VCO schematics shown in Fig. 1 are based on a differential Colpitts architecture first integrated in silicon at 1.5 GHz [6] and later scaled to mm-wave frequencies both in fundamental and in push-push VCOs [3,4],[7]-[9]. To further improve noise and design robustness, a number of developments borrowed from LNA designs are simultaneously applied. These include (i) differential cascode topology for improved tank isolation and power gain at mm-wave frequencies [3], (ii) inductive emitter degeneration [3], and (iii) resistive tail bias (as opposed to active current source bias) [10]. The 2nd-harmonic push-push VCO schematic shown in Fig.1.b employs an original topology which suppresses the fundamental oscillation and reinforces the

second harmonic signal. The output is collected from the bias node of the common-base output transistors, thereby providing improved isolation between the resonant tank and the load while allowing for a differential tuning voltage to be applied to the varactor diodes.

A novel, directly-modulated BPSK transmitter was implemented by integrating a mixing quad with a 65-GHz oscillator operating on the fundamental of the LC tank. The 1-2 GHz data signal is applied to the mixing-quad through emitter followers, as indicated in the schematic of Fig. 2.
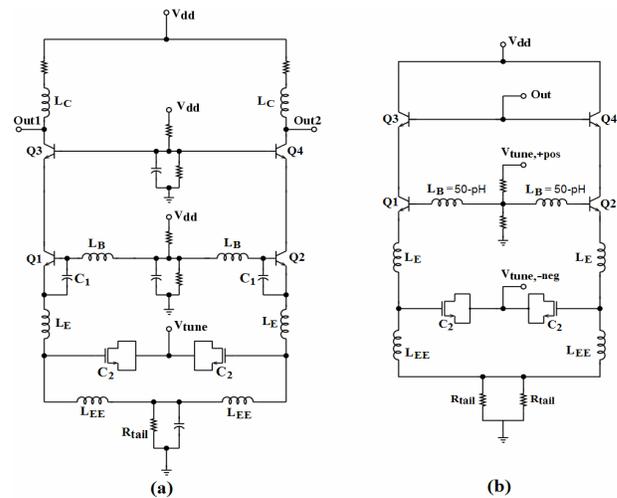

Figure 1. (a) 35-GHz VCO circuit schematic. (b) 120-GHz push-push VCO circuit schematic.
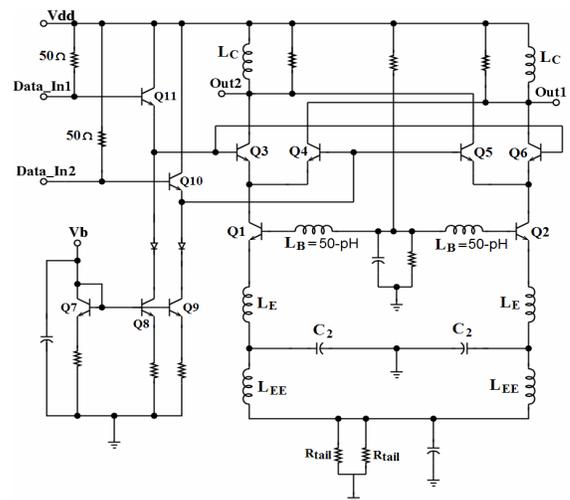

Figure 2. 65-GHz BPSK transmitter schematic.

LOW-NOISE DESIGN METHODOLOGY

The first step to achieving low phase noise is designing the highest quality factor (Q) LC-varactor resonant tank. As the Q of the resonant tank becomes strongly dependent on the varactor Q at frequencies above 30 GHz [7], the design of accumulation-mode n-MOS varactors for optimal Q becomes critical. Fig. 3 shows measured Q at 40 GHz for several interdigitated varactor geometries. These data illustrate that minimum gate width (to reduce gate resistance) and minimum gate length (to reduce channel resistance) are required to attain the highest possible Q. Fig. 4.a reproduces the measured 40-GHz Q and C-V characteristics of an optimized varactor with 10 fingers, each 180-nm long and 2.0-μm wide. It is comparable to the on-wafer measured Q of the multi-turn 80-pH inductor (Fig. 4.b) employed in the 70-GHz push-push VCO.

Even though a number of low phase noise mm-wave VCOs have been reported during the last two years, a systematic study and a design methodology for low-phase noise mm-wave VCOs has, to the best of the authors' knowledge, not been attempted yet. To that end, an algorithmic large signal design methodology was developed. It starts by setting the voltage swing across the resonant tank to the maximum value allowed for safe transistor operation (2.5 V_{p-p} for 35-GHz oscillators, and 2.0 V_{p-p} for 60-GHz oscillators) and by choosing the smallest inductor that can be reproducibly fabricated. Next, the transistors are biased at the optimum noise current density [1], as shown in Fig.5. Finally, the transistor and varactor size, and the capacitance ratio C_1/C_2, are scaled for minimum phase noise. Further phase noise improvement can be achieved by employing inductive emitter degeneration.

A set of eight 35-GHz VCOs and oscillators have been fabricated to experimentally validate the lowest phase noise design methodology. Fig. 6 compares the simulated and measured phase noise of 35-GHz and 60-GHz Colpitts fixed frequency oscillators as a function of tank inductance. Simulation and measured data are in good agreement and confirm the phase noise formula (1) from [11]. The latter describes VCO phase noise $S_{\Delta\varphi out}$ as a function of the equivalent noise current source $|I_n|^2$ representing all the noise contributions of the negative-resistance transistor, and of capacitors C_1 and C_2. The formula indicates that maximizing C_1 and the tank swing V_{01} will result in the lowest phase noise. Hence, the largest possible bias current (i.e. large transistors to simultaneously maximize C_1 and V_{01}) and the smallest tank inductance (to maintain a high LC resonant frequency) should be employed. Furthermore, the use of L_E as inductive degeneration consistently yielded ~0.5 dB improvement in phase noise according to simulations, and 3-4 dB improvement according to measurements, as seen in Fig. 6.

$$S_{\Delta\varphi out} = 2\frac{\left\langle |I_n|^2 \right\rangle}{|V_{01}|^2} \frac{1}{C_1^2 (C_1/C_2 + 1)^2} \frac{1}{\Delta\omega^2} \quad (1)$$

VCOs operating on the 2nd harmonic have the advantage of employing the LC-varactor resonant tank at half the oscillation frequency resulting in a higher tank Q. Anticipating the degradation of the tank Q at 60 GHz, operation on the second harmonic of 35-GHz and 60-GHz tanks was investigated to assess the optimal design trade-offs between low phase noise, broad tuning range, and output power.
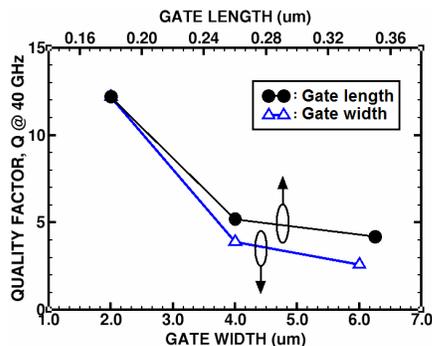
Figure 3. Measured worst-case-bias varactor Q at 40 GHz versus gate finger width and length.
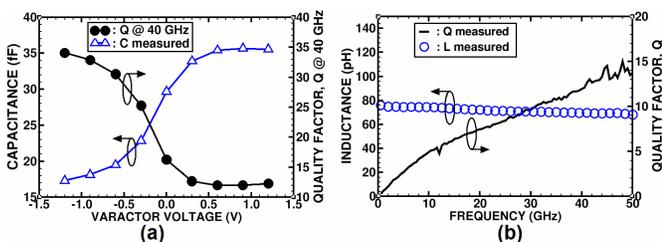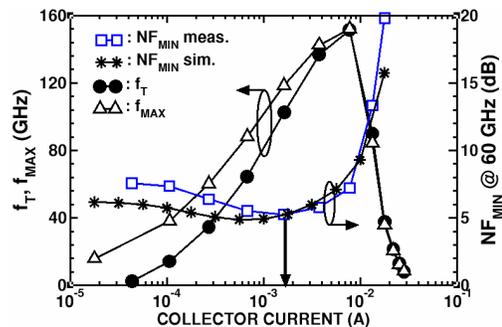
Figure 4. (a) Q-V & C-V characteristics of optimized varactor. (b) Q and L measurements of tank inductor used in 70-GHz push-push VCO.

Figure 5. Measured f_T, f_{MAX} and NF_{MIN} @ 60GHz of a 2 x 0.2 μm x 3 μm SiGe HBT.
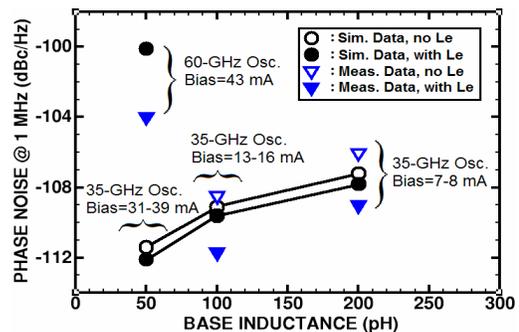
Figure 6. Simulation and measurement results exploring the lowest phase noise oscillator design space.

EXPERIMENTAL RESULTS

The circuits were fabricated in Jazz Semiconductor's SBC18 BiCMOS process which features f_T and f_{MAX} near 155 GHz (Fig. 5), and a collector-emitter breakdown voltage of 1.8 V. Photos of the 60-GHz VCO and BPSK transmitter are shown in Figs. 7.a and 7.b, respectively.

The area consumption of the 35-GHz, 60-GHz, 70-GHz, and 120-GHz VCO test structures is 525 x 475 μm^2, 485 x 475 μm^2, 420 x 450 μm^2, and 450 x 375 μm^2 respectively, including pads. The BPSK transmitter occupies 660 x 580 μm^2 including all 15 pads. An Agilent E4448A PSA with external Agilent 11970V and 11970W mixers were used for all V-band and W-band spectrum and phase noise measurements. The 35-GHz VCO outputs 1 dBm of power per side, has a phase noise of -110.3 dBc/Hz at 1-MHz offset, and 6.6 GHz (19%) tuning range. The corresponding metal-insulator-metal (MIM) capacitor oscillator exhibits a phase noise of -112.7 dBc/Hz (Fig. 8.a). The 60-GHz oscillator, which employs a MIM capacitor instead of a varactor, has a phase noise of -104 dBc/Hz (Fig. 8.b). The 60-GHz
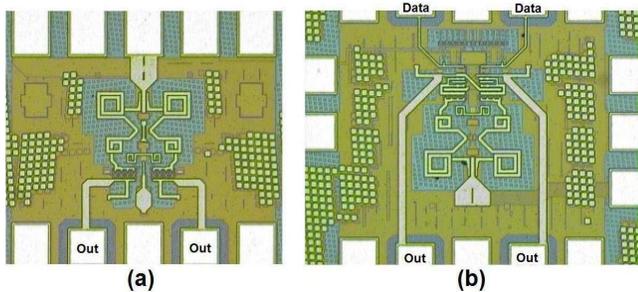
VCO, which operates on the fundamental of the L-varactor tank provides consistent output power (1 to -1 dBm) and wide tuning range (13% to 10.5%) over the 25°C to 125°C temperature range, as shown in Fig. 9.

Fig. 10 reproduces the measured tuning range of the 70-GHz and 120-GHz push-push VCOs of 15 GHz (21%) and 10 GHz (8.5%), respectively. The 70-GHz VCO output power reaches -14 dBm, and has phase noise of -94 dBc/Hz (Fig. 11.a). These values are pessimistic because cable, probe, and bias-T losses have only been measured up to 65 GHz and assumed to be constant above 65 GHz. Fig. 11.b reproduces the 120-GHz VCO spectrum showing an output power of -29.6 dBm. Again, the actual power is higher since the mixer conversion loss at 110 GHz, the bias-T, cable and waveguide insertion loss at 65 GHz have been used to de-embed the measured data. The 120-GHz VCO operates from a 4-V power supply and consumes 200 mW. Other VCO data are summarized in Table. 1.

Figs. 12 and 13 show the measured spectra of the BPSK transmitter when turning on and off the 1.5 GHz sinusoid that modulates the 65-GHz carrier. The transmitter operates from a 5-V power supply.

(a)   **(b)**

Figure 7. Microphotograph of (a) 60-GHz VCO and (b) 65-GHz BPSK transmitter.
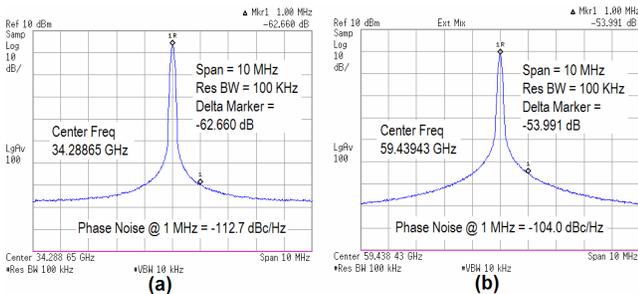

(a)   **(b)**

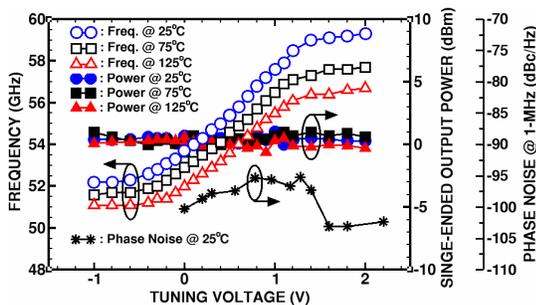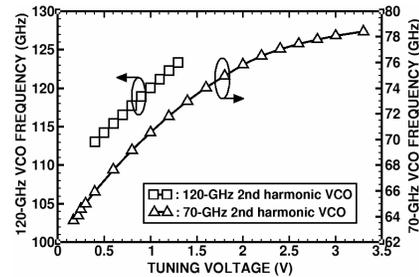Figure 8. Averaged spectral plot of (a) 35-GHz and (b) 60-GHz oscillators.

Figure 9. 60-GHz VCO output power & frequency over temperature and phase noise characteristics.

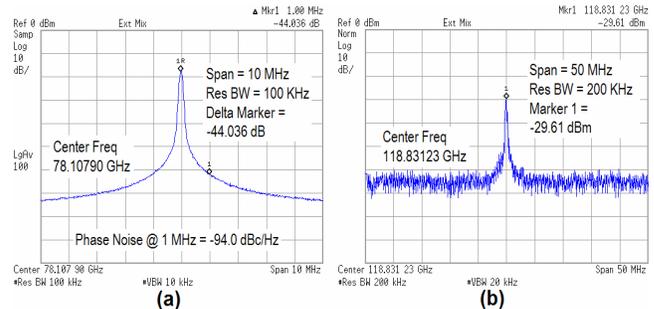Figure 10. Tuning ranges of 70-GHz and 120-GHz VCOs.

(a)   **(b)**

Figure 11. (a) 70-GHz VCO averaged spectral plot. (b) 120-GHz VCO spectral plot.
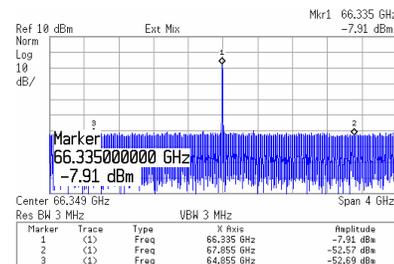

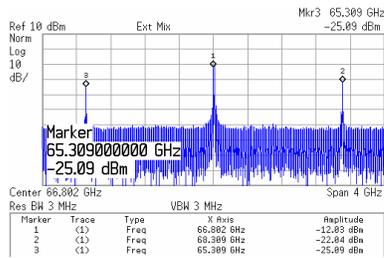Figure 12. 65-GHz BPSK transmitter spectrum without modulation.

Figure 13. 65-GHz BPSK transmitter spectrum with 1.5-GHz sinusoidal modulation.

CONCLUSION

A comprehensive simulation and experimental investigation of mm-wave SiGe HBT VCO design has demonstrated that phase noise improvement can only be achieved at the expense of increased bias current and reduced tank inductance. In 35-GHz and 60-GHz VCOs, the varactors degraded the phase noise by less than 2.5 dB when compared to MIM-capacitors, validating the effectiveness of accumulation-mode varactors in attaining wide tuning range with low phase noise. Inductive degeneration was experimentally found to improve the phase noise by 3-4 dB at identical bias but had negligible impact on the tuning range and output power. At the same time, the push-push designs exhibited typically 50% larger tuning range than that of fundamental mode VCOs, albeit at the expense of reduced output power. In addition, a compact directly-modulated 65-GHz BPSK transmitter has been successfully implemented.

ACKNOWLEDGMENTS

REFERENCES

[1] M. Gordon and S. P. Voinigescu, "An Inductor-Based, 52-GHz, 0.18 µm SiGe HBT Cascode LNA with 22dB Gain," accepted to ESSCIRC, 2004.

[2] M. Racanelli, et al., "SiGe BiCMOS Technology for Communications Products," *Proc. IEEE CICC*, pp. 331-334, Sep 2003.

[3] H. Li, et al., "Millimeter-Wave VCOs with Wide Tuning Range and Low Phase Noise, Fully Integrated in a SiGe Bipolar Production Technology," *IEEE J. Solid-State Circuits,* Vol. 38, pp.184-191, Feb 2003.

[4] Y. Baeyens, et al., "A Monolithic Integrated 150 GHz SiGe HBT Push-Push VCO with Simultaneous Differential V-Band Output," *IEEE MTT-S Digest,* pp.877-880, Jun 2003.

[5] T. Dickson, et al., "Si-Based Inductors and Transformers for 30-100 GHz applications," *IEEE Intl. Microwave Symp. Digest,* pp.205-208, Jun 2004.

[6] L. Dauphinee, et al., "A Balanced 1.5 GHz Voltage Controlled Oscillator with an Integrated LC Resonator, " *ISSCC Digest*, pp. 390-391, Feb 1997.

[7] S. P. Voinigescu, et al., "Family of Monolithic Inductor-Varactor SiGe-HBT VCOs for 20-GHz to 30-GHz LMDS and Fiber-Optic Receiver Applications," *RFIC Symp. Digest*, pp.173-176, Jun 2000.

[8] K. W. Kobayashi, et al., "A 108-GHz InP-HBT Monolithic Push-Push VCO with Low Phase Noise and Wide Tuning Bandwidth," *IEEE J. Solid-State Circuits*, Vol. 34, pp. 1225-1232, Sep 1999.

[9] H. Li, et al., "Fully Integrated SiGe VCOs with Powerful Output Buffer for 77 GHz Automotive Radar Systems and Applications Around 100 GHz," *GaAs IC Symp. Digest*, pp. 263-266, 2003.

[10] T. Johansen, L. Larson, "Optimization of SiGe HBT VCOs for wireless applications," *RFIC Symp. Digest*, pp. 273-276, Jun 2003.

[11] J.-C. Nallatamby, M. Prigent, "Phase Noise in Oscillators - Leeson Formula Revisited," *IEEE Trans. on MTT,* Vol. 51, pp.1386-1394, Apr 2003.

[12] N. Fong, et al., "A Low-Voltage 40-GHz Complementary VCO with 15% Frequency Tuning Range in SOI CMOS Technology, " *IEEE J. Solid-State Circuits*, Vol. 39, pp.841-846, May 2004.

[13] R.-C. Liu, et al., "63-GHz VCO using a standard 0.25µm CMOS process," *ISSCC Digest*, pp. 446-447, Feb 2004.

TABLE 1. Comparison of silicon-based monolithic mm-wave VCOs and oscillators

Reference VCO	f_{osc} (GHz)	L{f_{offset}} (dBc/Hz)	V_{DD} (V)	Tuning Range	P_{DC} (mW)	P_{OUT} (dBm)	FOM *	Technology
[3]	43	-110 at 1 MHz	-5.5	26%	280	6.5	-184.7	0.35 µm SiGe HBT
[4] push-push	150	-85 at 1 MHz	-6.5	23%	170	-5.0	-161.2	0.13 µm SiGe HBT
[7]	26	-87 at 100 KHz	5	15%	75	1.0	-177.5	0.5 µm SiGe HBT
[9]	77	-95 at 1 MHz	-5.5	6%	930	14.3	-177.3	0.35 µm SiGe HBT
[12]	40	-97 at 1 MHz	1.5	15%	17.3	-5.0	-171.7	0.13 µm SOI CMOS
[13] push-push	63	-85 at 1 MHz	1.8	4%	119	-4.0	-156.2	0.25 µm CMOS
This work: 35-GHz Osc.	34	-112.7 at 1 MHz	4.3	N/A	193	4.0	-184.5	0.18 µm SiGe HBT
This work: 35-GHz VCO	31	-110.3 at 1 MHz	4.5	19%	188	4.0	-181.4	0.18 µm SiGe HBT
This work: 60-GHz Osc.	59	-104 at 1 MHz	4	N/A	244	4.0	-179.5	0.18 µm SiGe HBT
This work: 60-GHz VCO	59	-103 at 1 MHz	4	13%	240	4.0	-178.6	0.18 µm SiGe HBT
This work: 70-GHz VCO push-push	78	-94 at 1 MHz	4	21%	128	> -14	< -156.8	0.18 µm SiGe HBT

* FOM = Figure of Merit = L{f_{offset}} - $20\log(f_{osc}/f_{offset})$ + $10\log(P_{DC}/P_{OUT})$